nature physics

INSIGHT | REVIEW ARTICLE

https://doi.org/10.1038/s41567-018-0107-y

The physics of cooperative transport in groups of ants

Ofer Feinerman[1]*, Itai Pinkoviezky[2], Aviram Gelblum[1], Ehud Fonio[1] and Nir S. Gov[3]

Anyone who has moved furniture together with friends will appreciate that cooperative transport requires some non-trivial communication. Yet ants are adept at collectively moving objects several times their size. How they do so has long been a subject of research, but recent advances have suggested that this communication occurs through the forces the ants exert on the load. This implies that the collective transport problem can be mapped to an Ising model, in which decisions by individual ants are described by spin flips. Within this framework, the group is poised in the vicinity of the transition between uncoordinated and coordinated motion. It thus profits from both internal coordination and maximal responsiveness to external information, mediated by temporarily informed leader ants. Here, we review the implications of these findings for cooperative transport, and discuss the way in which a more complete multiscale understanding of such systems would require the development of a new formalism that combines statistical physics of interacting particles with the cognitive capabilities of individuals.

The mesmerizing collective displays exhibited by animal groups such as flocking birds or schooling fish have attracted the attention of the physics community for several decades[1–7]. Research has revealed that these groups share a large number of characteristics with interacting many-particle physical systems, including long-range order from short-range interactions[4], travelling waves[8], broken symmetries[9], self-organization[10] and various collective states[5,9,11]. The interactions between the individuals in a group rely on visual[12,13], tactile[14,15], hydrodynamic[16], chemical[17–19] and auditory[20,21] communication, or a combination of these cues. However, it is often difficult to deduce exactly which of the available stimuli are actually used by the animals[4,22].

One group behaviour in which the interactions are potentially more straightforward is cooperative transport, as it fundamentally relies on the application and sensation of mechanical forces. Cooperative transport occurs when a group of animals join forces to carry a large object[23,24]. Most animal species do not display this skill, humans and a number of ant species being some of the rare exceptions[23]. Ants employ cooperative transport (Fig. 1a) to exploit resources from their environment and overcome competition[23,25]. They have been known to collectively transport food weighing over 5,000 times the weight and 10,000 times the volume of a single worker[26].

A first condition towards moving such large items is that the ants gather enough muscle power to lift or drag[27,28] the load[26,29,30]. Summoning enough ants is a necessary condition towards moving heavy loads but it is in no ways sufficient. Efficient transport requires that group members coordinate their forces rather than engage in futile tugs-of-war[27,31]. Indeed, it has been suggested that during the collective motion the carrying ants align their pulling efforts[23,26]. As an ant connects to a cooperatively transported load, she is inevitably exposed to and affected by the stream of information conveyed by the forces applied to her at her point of contact[23,32–35]. Ants may use this information to coordinate their pulling directions.

Although getting a large load to move is a prerequisite for successful transport, steering it in the correct direction is no less important. The collective decision regarding the direction of motion is reflected by the angle of the vector sum of all forces applied by the ants and is therefore readily measurable from the kinematics of the load's motion. Measurements of load trajectories have revealed that the carrying group can be in one of several collective states that include deadlock, uncoordinated motion and fast directed motion[27]. Until recently, the origins of these dynamical modes, reminiscent of the different collective patterns of motion observed in flocking animal groups[5,9,11], and their relations to steering and eventually successful navigation have not been fully understood.

The sheer number of ants involved in these collective efforts make them amenable to tools such as rate equations[36] and statistical mechanics, much like those used to describe flocking[37]. It has been proposed that starling flocks and midge swarms exhibit characteristics that are known to be associated with criticality in large physical systems[38], such as long-range and scale-free spatial correlations[39]. It was further suggested that individuals in these systems self-tune their interaction strength such that criticality can be maintained over a range of different group sizes[40,41]. Such dynamic tuning may make it difficult to experimentally transition these systems through their critical point. It has been further speculated that residing near a critical point may be advantageous for a moving animal group because high susceptibility could translate to increased responsiveness to external stimuli[42]. This, however, has yet to be shown[39].

The recent rise in computing power, combined with the development of high spatio-temporal-resolution cameras, has allowed the acquisition of large, detailed data sets that track individuals during the collective transport process (Fig. 1b). Combining data analyses with theoretical modelling can yield new insights into the process of cooperative carrying by ants, revealing the microscopic rules employed by individual ants and the means by which their behaviours lead to the emergence of collective motion.

In what follows, we outline several works that employ the tools of statistical mechanics and dynamical systems to study cooperative transport in the longhorn crazy ant (*Paratrechina longicornis*). We demonstrate that these tools can be used to undertake quantitative analysis, and predict new qualitative features of the transport process. Although different ant species may utilize different mechanisms for cooperative transport[23,28,29,33,43], we demonstrate how physics-based modelling can assist in finding similarities between different species and, ultimately, enhance our understanding of the ecology and evolution of social insect cooperation.

Ordered states and forceful cooperation

P. longicornis performs impressive cooperative transport[33,34,44–47]. The load trajectories are relatively smooth despite the frenzied, erratic

[1]Department of Complex Systems, Weizmann Institute, Rehovot, Israel. [2]Departments of Biology and Physics, Emory University, Atlanta, Georgia, USA. [3]Department of Chemical and Biological Physics, Weizmann Institute, Rehovot, Israel. *e-mail: ofer.feinerman@weizmann.ac.il

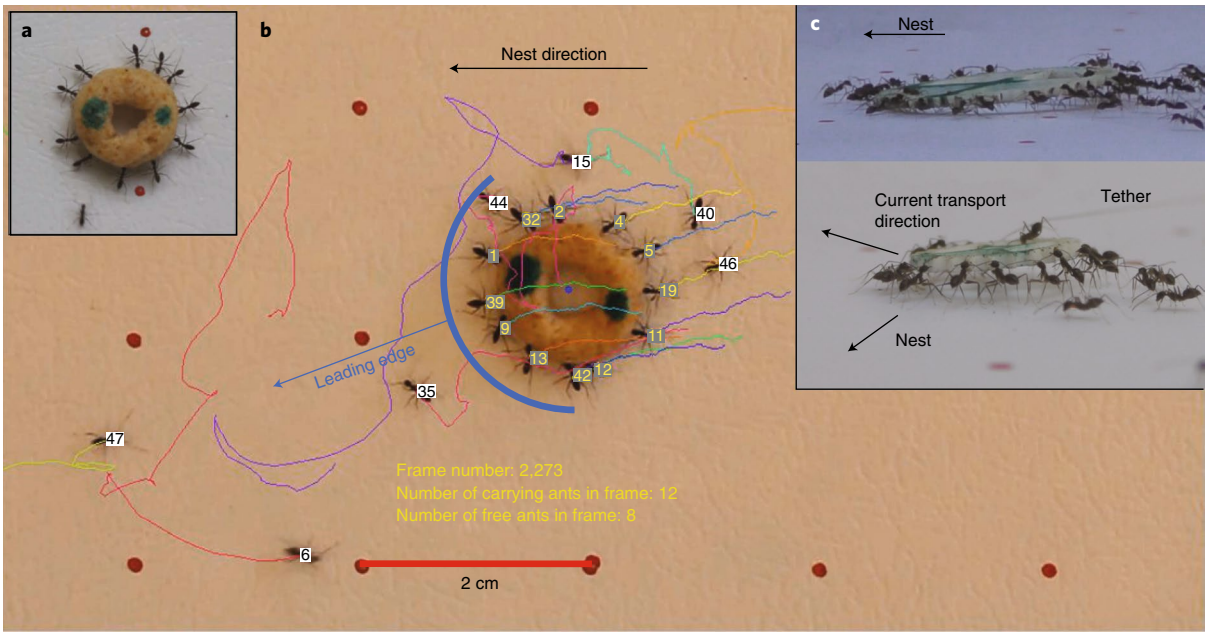

Fig. 1 | Cooperative transport. a, A team of *P. longicornis* ants retrieving a large food item. **b**, Snapshot from a tracked movie. The yellow and black numerals denote carriers and non-carriers, respectively. The object's current direction of movement is depicted by the blue arrow. Scale bar, 2 cm. **c**, Side view of cooperative transport. The distribution of puller ants in the leading edge and lifters in the trailing edge causes the load to slant in the direction of transport, whether it is towards (top panel—free motion) or perpendicular (bottom panel—constrained motion) to the nest direction.

activity of the surrounding ants and the high rate of joining and detaching. An efficient strategy for probing the mechanisms that enable this coordination is to study the collective performance as a function of group size. This is achieved by using ring-shaped loads of different radii that attract different group sizes while maintaining the mass per carrying ant roughly constant. Interestingly, larger groups exhibit smoother motion, characterized by trajectories with longer persistence length[33] (Fig. 2a).

In this overdamped system, speed is directly proportional to the total force[33]. Therefore, to achieve efficient transport, the forces applied by individual carriers must be aligned. This alignment could be realized by uncoupled carriers that independently align their force toward the nest[23,36]. Conversely, alignment could be achieved by communicating ants that actively attempt to match their actions with those of their fellow carriers[33]. In this second case, an ant is not required to know the direction to the nest, but rather attempts to align its force with the current direction of motion. These two basic alignment mechanisms differ in the requirements they place on individual capabilities and also in the resulting collective motions.

The uncoupled-carriers model provides a possible explanation for the association between larger groups and smoother trajectories. Here, inaccuracies in the direction of forces applied by different individuals are uncorrelated. The motion of the load is determined by the sum of all these forces such that independent noise terms cancel out and accuracy increases with group size. This polling effect, termed the 'many-wrongs principle' or 'wisdom of the crowd', has been suggested as an accuracy-enhancing mechanism in flocking motion[48] and human decision-making[49,50].

The basic realization of the coupled-carriers model assumes that ants are coupled to each other exclusively via the force each ant senses at her point of attachment to the carried load[33] (see Box 1). The physiological mechanisms that allow for this force sensing are currently unknown and remain a challenge for future research. For a rigid load, this assumption implies that each ant reacts to the sum of all the forces ($\mathbf{F}_{\mathrm{tot}}$) applied to the cargo by the carrier ants and this leads to a fully connected model. The sign of the interaction is such that ants in the leading edge of the load tend to pull and those at the trailing edge tend to lift and reduce friction (Figs. 1c and 2b). The strength of these tendencies can be captured in the following mathematical form for the rates at which carrier ants switch between these two possible roles.

$$r_{\mathrm{l}\to\mathrm{p}} = K_{\mathrm{c}} \mathrm{e}^{\frac{\hat{p}_i \cdot \mathbf{F}_{\mathrm{tot}}}{F_{\mathrm{ind}}}}$$
$$r_{\mathrm{p}\to\mathrm{l}} = K_{\mathrm{c}} \mathrm{e}^{\frac{-\hat{p}_i \cdot \mathbf{F}_{\mathrm{tot}}}{F_{\mathrm{ind}}}} \quad (1)$$

where K_{c} is the basal decision-making rate of individual ants, $\hat{p}_i$ is the unit vector along the body axis of ant i and F_{ind}^{-1} is a coupling parameter that sets the force scale for the alignment interaction. The particular choice of Boltzmann factors for these rates enables the use of a thermodynamics treatment, as shown below. A similar formalism was used to describe the collective motion of molecular motors[51,52].

Equation (1) implies that when $F_{\mathrm{tot}} \gg F_{\mathrm{ind}}$, an ant will align her own pulling force with the total force (or lift if attached to the trailing edge). Conversely, when $F_{\mathrm{tot}} \ll F_{\mathrm{ind}}$, the ants randomly pull or lift. In behavioural terms, a large F_{ind} corresponds to high individuality, and a small F_{ind} corresponds to conformity. Therefore, since the total force sensed by the ants grows with the number of carriers, ants in larger groups will actively coordinate their forces whereas those in smaller systems will remain uncoordinated. Hence, in this model, smooth trails for large group sizes (Fig. 2c) are the result of an increase in the internal coordination between the ants.

Although both the coupled and the uncoupled models provide a possible explanation for the relation between group size and trajectory smoothness (Fig. 2a), they disagree on the expected speed profiles. In the uncoupled-carriers model, the mean speed of the cargo is proportional to the sum of all individual ant forces

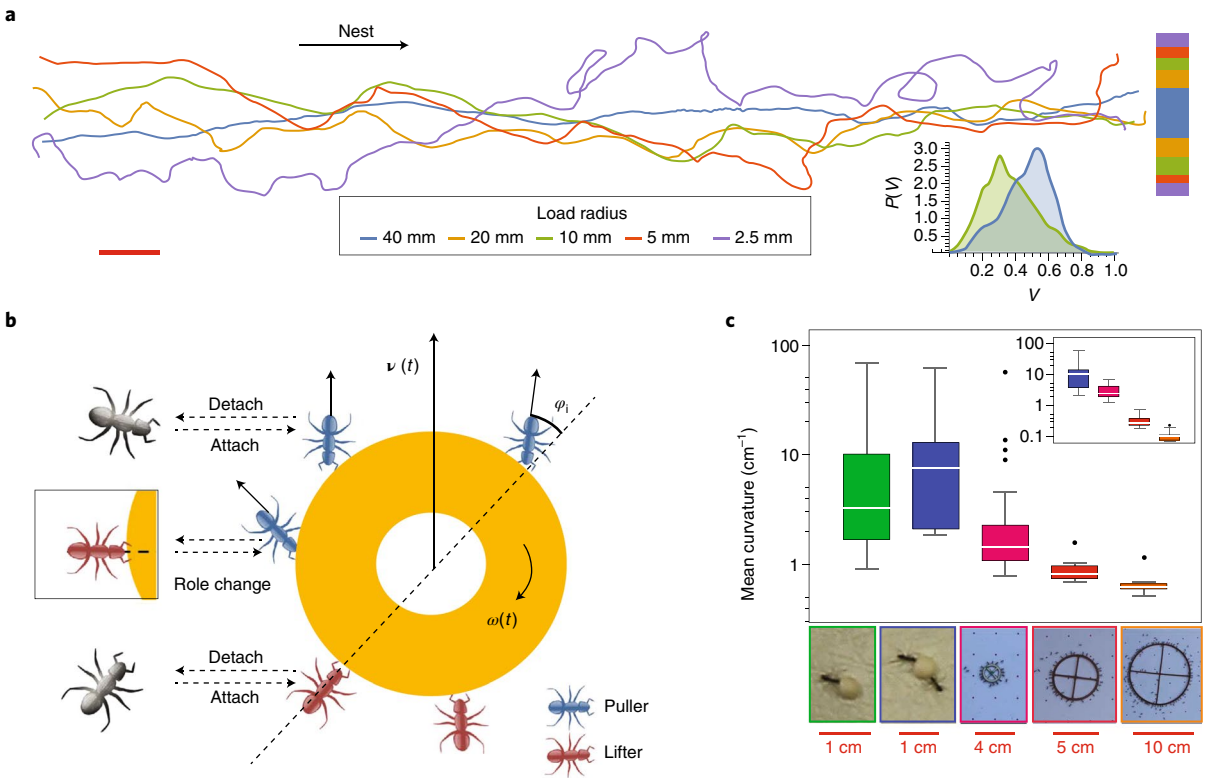

Fig. 2 | Empirical findings and theoretical model. a, Sample nest-bound trajectories for various load sizes (red scale bar, 5 cm). The maximal amplitude along the *y* direction for each trajectory is depicted by the right bar with the same colour code as the trajectories. The inset shows the speed probability density functions for two load sizes (R=10, 40 mm). **b**, A schematic diagram of the coupled-carriers model indicating the possible transitions for non-informed ants. For further details, see Box 1. **c**, Mean absolute curvature of trajectories of objects of different sizes (radius). Inset: median curvature of tracks obtained by simulating the model presented in **b** for objects of different sizes (radii). The number of carrying ants scales with the radius of the ring-like objects. The curvature was calculated by fitting second-order polynomials to spline fits of the segmented trajectory. The standard box-plot representation includes a coloured box (interquartile range, Q1 and Q3), median value (Q2, white horizontal line inside the box), whiskers extend to the last datum still within 1.5 times the interquartile range from either below Q1 or above Q3. Further data are considered as outliers and are represented as black dots.

normalized by object mass, which, for ring-shaped loads, is proportional to the number of ants. In other words, collective speed is proportional to the mean force over all individual ants. By the law of large numbers, we expect this speed to be independent of group size, whereas fluctuations decrease for larger groups. Conversely, the coupled-carriers model predicts that larger systems display stronger alignment, with fewer tug-of-wars and therefore higher collective speeds. Experimental results (see Fig. 2a, inset) support the prediction of the coupled-carriers model.

In the coupled-carriers model, group motion is initiated through random fluctuations in the roles of the ants that are attached to an immobile load ($\mathbf{F}_{\mathrm{tot}}=0$ in equation (1)). A large enough fluctuation leads to a net total force that, in turn, induces coordination[33] (finite $\mathbf{F}_{\mathrm{tot}}$ in equation (1)). However, as motion commences, carrier ants simply amplify the current direction regardless of how well it is aligned to the nest. Next, we show how physical principles help the ant group overcome this difficulty such that the motion is indeed directed towards the nest.

Criticality and ant leadership

The coupled model displays a transition between random-like motion (a 'tug-of-war') to more ballistic trajectories, as a function of group size (Fig. 2a,c). Interestingly, fitting the model's parameters so that the resulting collective behavior matches the features of the measured motion (see Box 1) reveals that groups within the naturally relevant size range fall in the transition area between these two regimes (see the insets of Fig. 3a). Next, we explore the relevance of this observation to the group's ability to correctly navigate towards the nest.

The transition between random and ballistic motion is reminiscent of order–disorder transitions in statistical mechanics and can be theoretically explored using a simplified coupled model for a load that moves along one dimension (Fig. 3b). Here, N ants carry an object with a front and a back such that $N/2$ of them are located on each edge. This model can be mapped to a fully connected Ising model, where the role of each ant is depicted by a 'spin' degree of freedom, and $\sigma_i=0$, 1 denotes either a lifter or a puller. The translational invariance of this model, together with the choice of Boltzmann transition rates between puller and lifter roles (see equation (1)), implies that this inherently non-equilibrium, dissipative system can nevertheless be described by an effective equilibrium steady state. One can therefore define the following Hamiltonian

$$H=-\frac{f_0}{F_{\mathrm{ind}}}\sum_{i\neq j}p_i p_j \sigma_i \sigma_j \qquad (2)$$

where f_0 is the pulling force applied by a single ant and $p_i=+1, -1$ denotes either the right or left side of the load, respectively. The interactions between ants on the same side are ferromagnetic, whereas those between ants on opposite sides are antiferromagnetic. Taking

Box 1 | Description of the theoretical model

Here, we describe the theoretical model of coupled-carriers (Fig. 2b) as implemented in the numerical simulations[33,34].

Attachments–detachments of carrying ants. The circular cargo is divided into N_{max} equally spaced sites labelled by the angle θ_i, $i \subset [1, N_{max}]$. A site can be empty or occupied by either a puller or a lifter. The cargo is surrounded by a reservoir of ants from which ants attach to the cargo at a constant rate K_{on}. Attached ants detach at a rate K^i_{off} (at site i), which was found to depend on the motion of the cargo: when the cargo is stationary the detachment rate is higher than the rate when the cargo is moving.

Role switching. An attached ant can assume either a pulling or a lifting role. A puller ant contributes to the cargo's velocity by applying a force along her body axis. To maximize her effect, the puller ant aligns as closely as possible with the direction of the total force that it senses. The angular range of this tilt angle (denoted as φ_i), with respect to the local radial direction (Fig. 2b), is limited to a window of angles: $[-\varphi_{max}, +\varphi_{max}]$. Lifter ants simply lift the cargo to reduce the normal force and therefore the friction by a factor β. Lifters are assumed to be oriented radially, so that their tilt angle is zero ($\varphi_i = 0$).

The basic assumption of the model is that the probability to be a puller/lifter depends on the ant's location around the load, her local tilt angle and the current direction of motion, and is determined by the switching rates specified in equation (1). Each ant reacts to a combination of the total force on the centre-of-mass ($\mathbf{f}_{cm}$) and the torque, which depends on her point of attachment:

$$\mathbf{F}^i_{tot} = \mathbf{f}_{cm} - \mathbf{f}^i_{rot} \tag{8}$$

$$\mathbf{f}_m = \mathbf{f}_0 \sum_{i=1}^{N_{max}} n^i \hat{p}_i - \mathbf{f}_{kin} \tag{9}$$

$$\mathbf{f}^i_{rot} = \frac{\gamma_{rot}}{b} \mathbf{r}_i \times \boldsymbol{\omega} \tag{10}$$

where $n^i = 1, 0$ if site i is occupied with a puller/lifter respectively, $\hat{p}_i = \cos(\theta_i + \varphi_i), \sin(\theta_i + \varphi_i)$ is the body axis vector of the ant at the ith site, f_0 is the magnitude of the force applied by a single puller, $\mathbf{f}_{kin}$ is the kinetic friction (with τ_{kin} as the kinetic friction torque), b is the outer radius of the object ($b = |\mathbf{r}_i|$) and $\boldsymbol{\omega}$ is the angular velocity that is given below. Note that the negative sign in equation (8) induces the puller ants to orient as to oppose the rotation force $\mathbf{f}^i_{rot}$.

Finally, the contribution of the lifter ants to the motion is through the friction term $\mathbf{f}_{kin}$. Its magnitude is given by

$$f_{kin} = \max\{f^0_{kin} - \beta N_{lifters}, 0\} \tag{11}$$

where f^0_{kin} is the bare friction force, β is the reduction in friction due to a single lifter and $N_{lifters}$ is the number of attached lifters. When there are enough lifters such that $f_{kin} = 0$, additional lifter ants do not affect it further.

Equations of motion of the cargo. When the puller ants overcome the static friction, the velocity of the centre of mass $\mathbf{V}_{cm}$ and the angular velocity ω are given by:

$$\mathbf{V}_{cm} = \frac{\mathbf{f}_{cm}}{\gamma} \tag{12}$$

$$\omega = \frac{f_0 \sum_{i=1}^{N_{max}} n^i \sin(\varphi_i) - \tau_{kin}}{\gamma_{rot}} \tag{13}$$

where γ is the cargo response coefficient, which is proportional to the mass of the object, and γ_{rot} is the response coefficient for an applied torque.

The model dynamics are stochastic, involving rates for a variety of random processes, such as attachment, detachment, reorientation of pullers and role change. These dynamics were implemented in a stochastic simulation, using a Gillespie algorithm[81]. In each iteration, the time to the next event is drawn according to the total rate of all the possible reactions.

Parameter fitting. Although the coupled model has many parameters, only four of them are free in the sense that they are not directly measurable[33]. The number of free parameters is small when compared to the large number of dynamical features that could be extracted from the ants' collective motion. Fitting can be performed by using control experiments in which informed ants are not allowed to approach the load[33]. In this way, all participating ants are uninformed, and can be assumed to behave according to the rules of the coupled model.

the limit $N, F_{ind} \to \infty$, while keeping $\tilde{F}_{ind} = F_{ind}/N = \text{const.}$ yields the exact mean-field solution to this Hamiltonian (at temperature $T = 1$)

$$\frac{F_{tot}}{N} = \frac{f_0}{2} \tanh\left(\frac{F_{tot}}{F_{ind}}\right) \tag{3}$$

where $F_{tot} = f_0 \Sigma p_i \sigma_i$ is the order parameter. This model undergoes a second-order phase transition (Fig. 3c), such that below the critical point ($\tilde{F}_{ind,c} = 0.5$), the order parameter $F_{tot} \propto N$, whereas above it $F_{tot} \approx 0$. Note that the critical point can be approached by varying either F_{ind} or, the more experimentally accessible, N, as these are inversely related.

The mean-field solution (equation (3)) is exact in the thermodynamic limit, where fluctuations around the equilibrium state vanish. Nevertheless, simulations reveal that the order–disorder transition remains evident even for finite-size systems[41], containing as few as $N = 10$ carriers (Fig. 3c). Experimentally varying the size of the load (and carrying ant group, N) yields qualitative agreement with Fig. 3c: larger objects move at higher speeds (Fig. 2a inset). The dependence of speed on group size is particularly clear when considering a scenario that includes an external constraint (see below).

Second-order phase transitions are characterized by a divergence in the susceptibility at the critical point. This raises the tantalizing possibility that the ant group may exploit this property to address the navigational challenge of steering towards the nest. One way to implement a small external field in the analytical model is by including a single 'uncoupled' ant (analogous to a zealot spin[53,54]) that persistently pulls in a fixed direction while

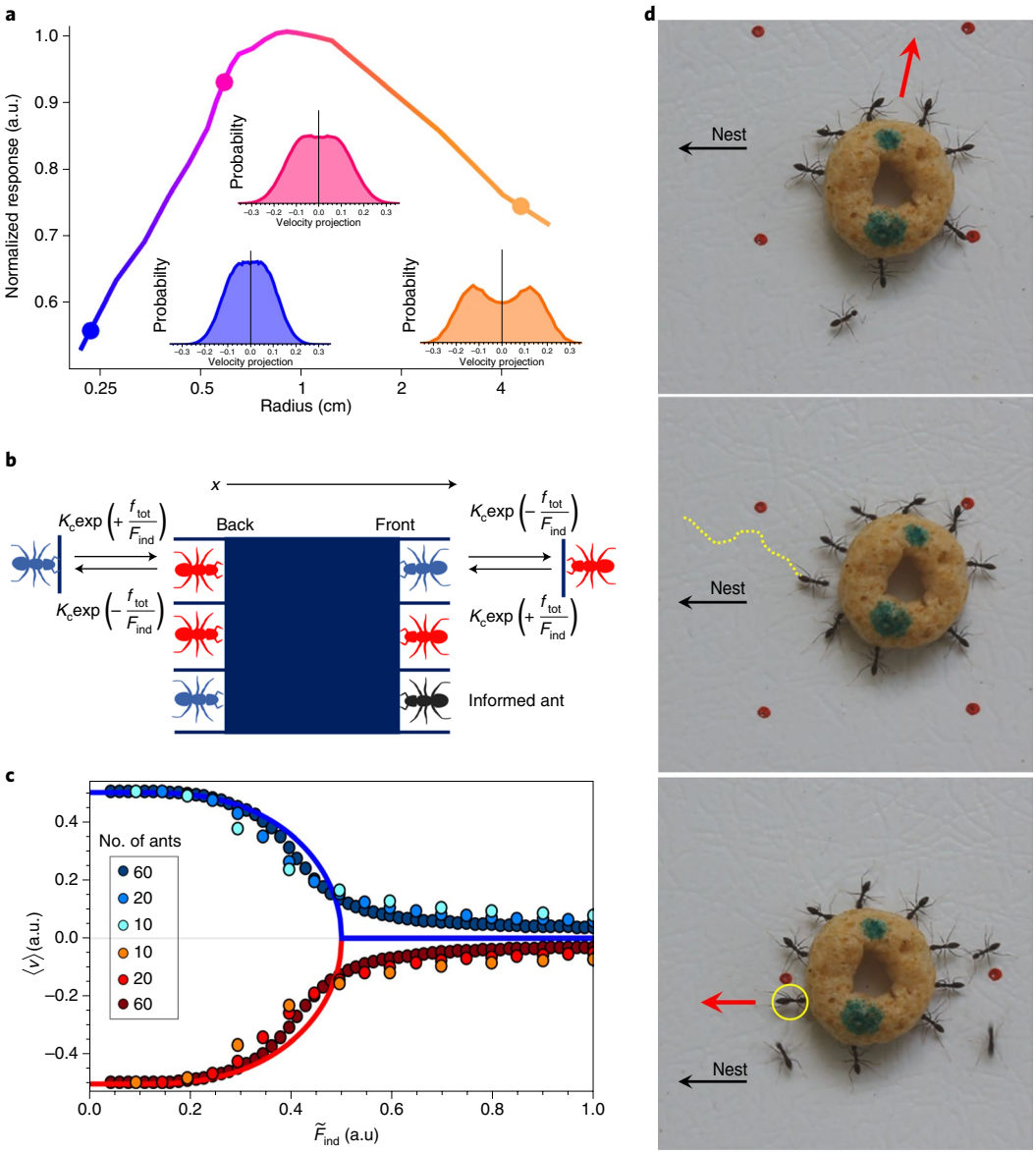

Fig. 3 | Criticality, susceptibility and leadership. a, The curve depicts the simulated response of the object to a single attachment of an informed ant as a function of the object's radius (normalized by the maximal calculated value). The response is defined as the mean speed at which the group moves in the direction of the nest, following the attachment of a single informed ant. The insets depict simulated (see model in Fig. 2b) velocity projection distributions for large (orange), medium (pink) and small (blue) loads. These distributions correspond to ballistic (ordered), transition regime and random-walk (non-ordered) motions, respectively. **b**, An illustration of the simplified coupled model that takes the form of a fully connected Ising model. The motion is one-dimensional moving along the *x* direction. Blue and red ants as in Fig. 2b. Non-informed ants change their roles while the leader ant (black) remains a puller. **c**, Mean velocity of the one-dimensional motion calculated using the simplified coupled model plotted against the renormalized coupling parameter: $\tilde{F}_{ind} = F_{ind}/N$. The solid curves are the analytical solutions of the mean-field equation while the circles represent averages obtained from simulations with different group sizes, *N*. **d**, Group of ants transport a load in the wrong direction (top). The instananeous direction of motion is indicated by the red arrow. An informed individual (marked in yellow) arrives at the load (middle). The group reacts to the attachment of the informed leader (encircled in yellow, bottom) by aligning the transport direction with the nest direction (bottom).

ignoring any forces applied by others. The direct analogy with the Ising model implies that, at the critical point, the entire group of coupled carriers will tend to maximally align with this persistent puller. An uncoupled ant pulling in a constant direction can also be included into the full version of the coupled-carriers model (Box 1). Simulations show that the group indeed reorients its collective direction such that it tends to align with the pulling direction of the uncoupled ant. This response is maximized for groups that carry naturally sized loads (Fig. 3a), which places them near the order–disorder transition (Fig. 3a insets). Finally, we note that the inclusion of uncoupled ants in the coupled-carriers model slightly blurs the clear distinction between the coupled and uncoupled descriptions, as stated above.

Experimentally, it is known that freely moving ants are extremely well oriented and are able to return to the nest from large distances[55]. *P. longicornis* ants are no exception: during cooperative transport, non-carrying ants integrate their own memories of the environment with information conveyed by the scent marks left by others to learn about the correct route towards the nest[33,47]. It is further known that informed ants tend

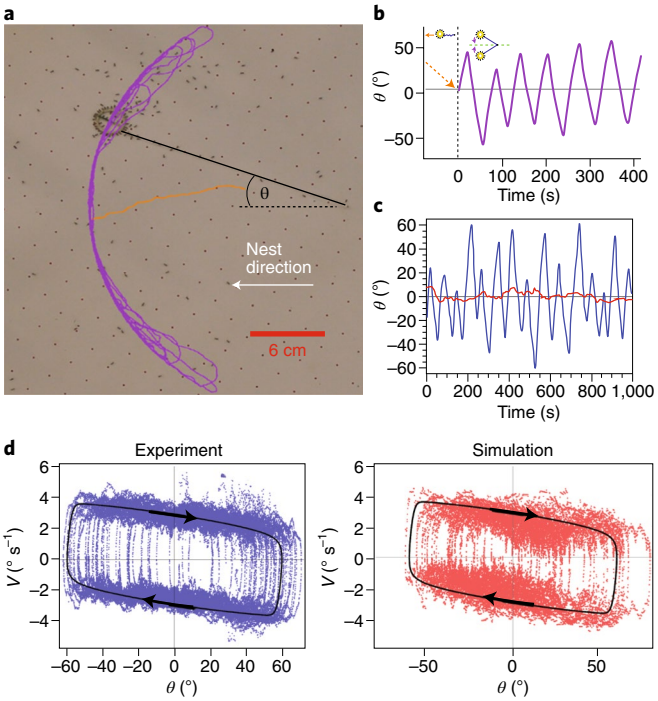

Fig. 4 | Oscillatory motion under constrained conditions. a, The motion of cooperatively carrying ants when constrained by a thin tether (black line). Free motion before encountering the constraint is marked in orange while oscillations, when the string is fully taut, are marked in purple. **b**, Time series of the load's motion. A black dashed line separates the two stages of motion described above. The angle, θ, is measured relative to the direction of the nest. **c**, Comparison between a coupled model that contains both informed and non-informed ants (blue curve) and an uncoupled model that includes only noisily informed ants (red curve). The uncoupled model fails to reproduce the experimentally observed oscillations. **d**, Phase space of oscillation data (experimental measurements in blue, coupled model simulations in red) of the angle around nest direction (θ) and the corresponding angular velocity. The black line depicts the analytic result for the limit cycle obtained from the constrained version of the simplified coupled model (Fig. 6a).

to ignore social information and act independently from other group members[56]. It is therefore interesting to check the effect that a newly attached ant may have on the collective motion. In agreement with the theoretical results mentioned above, experiments show that, on attachment, such ants are able to steer the entire carrying group towards the nest (Fig. 3d). This leadership effect[57,58] is short-lived—the boost in the directional information that the leader provides to the group dwindles after about 10 s. This most likely occurs as the leader ant loses her initial informational edge over the other carriers[33]. Updated information continues to flow into the system by the constant flux of attaching ants.

To summarize, the carrying ants appear to be coupled through mechanical forces and this leads to a high degree of coordination with minimal force cancellations (see the inset of Fig. 2a and ref. [33]). As mentioned above, a downside of this is that carrying ants direct their attention within the group and not towards their surroundings. Balancing individuality and conformism offers a compromise that helps solve this problem. It allows the ants to be relatively strongly aligned, while maintaining high susceptibility to the directional information conveyed by transient leader ants.

External constraints and swinging modes

A clear distinction between the coupled-carriers and uncoupled-carriers models is the location of pullers and lifters along the circumference of the load. In the coupled model, the ants organize relative to the current direction of motion: puller ants reside in the leading edge of the load, whereas lifters occupy the trailing edge. Conversely, in the uncoupled model, the pullers are along the edge of the load facing the nest and lifters along the edge facing away from the nest. During unconstrained movement (see the previous section), these differences may be difficult to distinguish as the motion is typically aimed towards the nest. Constraining the motion, for example by tethering the carried load with a thin string (Fig. 4a), can decouple the direction of allowed motion from the direction to the nest[34].

P. longicornis ants carrying tethered cargoes were found to exhibit large-amplitude oscillations around the direction of the nest (Fig. 4b). These shark-fin-shaped oscillations are highly periodic, which is surprising given the large stochasticity on the level of individual ants.

During the sideways oscillatory motion, puller ants can be observed to occupy the leading edge of the load, whereas lifters occupy its trailing edge, regardless of the direction to the nest (Fig. 1c, bottom panel). This supports the coupled-carriers model, wherein the majority of ants are uninformed about the direction to the nest and tend to align their forces according to interactions within the group. Clearly, the observed oscillations could not arise from a wisdom-of-the-crowd-type mechanism, as suggested by the uncoupled-carriers model (Fig. 4c, red plot).

The constrained system was modelled using the same coupled model described in the previous section, except for the addition of a tether as a Lagrangian multiplier[34]. Newly attached, informed ants are assumed to always pull in the direction of the nest. The model quantitatively captures multiple aspects of the cargo's motion (Fig. 4c, blue plot, and Fig. 4d) such as the angular speed, oscillation amplitude and period-to-string-length relation[34].

The coupled model also predicts dynamical transitions between order and disorder (Fig. 5, top panel), which could be experimentally tested by varying group size. Specifically, the model predicts that oscillations disappear for small group sizes, for which only random motion of the cargo around the direction of the nest is observed. In addition, it was predicted that larger objects should oscillate with longer periods. These two predictions have been experimentally verified (Fig. 5, bottom panel), providing strong support to the idea that the oscillatory motion is a collective emergent behaviour.

Unlike the free system, the tethered configuration lacks translational invariance and this reveals its inherently non-equilibrium nature. Above the ordering transition, a non-zero speed, v, appears. When this is combined with the broken translational symmetry, as dictated by the tether, it results in broken time-reversal symmetry. This broken symmetry is manifested as relaxation oscillations of the order parameter along a limit cycle (Fig. 4d). We note that these properties of the ant model are shared by a class of non-equilibrium, driven-dissipative condensed-matter systems. These exhibit similar many-body transitions into a state with broken time-reversal symmetry, periodically varying Hamiltonians and limit-cycle dynamics[59,60].

The dynamics of this non-equilibrium system can be analysed using nonlinear ordinary differential equations derived from the simplified coupled model, described in the previous section, in which the cargo is constrained to move on a circle with fixed radius, L (ref. [34] and Fig. 6a). The two variables in this model are (θ, v), the angular displacement and tangential speed, respectively. The equations of motion are:

$$\frac{\mathrm{d}\theta}{\mathrm{d}t} = \frac{v}{L}$$

$$\frac{1}{K_c}\frac{dv}{dt} = -\frac{\widetilde{G}}{K_c L}v\cos(\theta) + \tilde{N}\sinh\left(\frac{v}{\widetilde{F}_{ind}}\right) - 2\left(v + \widetilde{G}\sin(\theta)\right)\cosh\left(\frac{v}{\widetilde{F}_{ind}}\right) \quad (4)$$

where $\tilde{N}$ is proportional to the total pulling force of the uninformed ants, $\widetilde{G}$ is proportional to the total force the informed ants exert towards the nest, $\widetilde{F}_{ind}$ is the individuality parameter normalized by the size of the load and v is proportional, as above, to F_{tot}.

Linearizing the speed equation in equation (4) in the variable v, we get

$$\frac{1}{K_c}\frac{dv}{dt} = \left(\frac{\tilde{N}}{\widetilde{F}_{ind}} - 2 - \frac{\widetilde{G}}{K_c L}\right)v - 2\widetilde{G}\sin(\theta) \quad (5)$$

where, in the second term, the force exerted by informed ants acts as a 'gravitational' force. The first term defines an effective friction coefficient. For a small uninformed population, the friction term is negative and tends to decrease the speed and stabilize the fixed point at $v=\theta=0$. When the number of uninformed ants surpasses the threshold given by

$$\tilde{N}_c = \widetilde{F}_{ind}\left(2 + \frac{\widetilde{G}}{K_c L}\right) \quad (6)$$

the friction term switches its sign and provides positive feedback that gives rise to the oscillatory behaviour. An analysis of the system's eigenvalues shows that the origin undergoes a Hopf bifurcation at the critical value specified by equation (6). This threshold agrees with the simulation and experimental results as presented above (Fig. 5). Interestingly, this transition can spontaneously occur under natural conditions in which the group's motion is delayed by an obstacle[34]. As time goes by and more ants are recruited to the object, the system can naturally go into its ordered phase and commence a sideways motion that assists obstacle circumvention[34,46].

When the number of ants is large, the simplified model enters an ordered regime, dominated by the nonlinear terms in equation (4). In this regime, there is a strong separation of timescales where, most of the time, the cargo moves with nearly constant speed such that $dv/dt \approx 0$ (see shark-fin oscillations in Fig. 4b). One can therefore use equation (4) to define an effective free energy $W(v,\theta)$ (Fig. 6b) whose minimum sets this slowly changing speed

$$\frac{dv}{dt} = -\frac{dW(v,\theta)}{dv} \approx 0 \quad (7)$$

The physical origin of the oscillations can now be explained by a Landau-like mechanism, where v acts as the order parameter. Unlike an equilibrium Landau description, here a non-zero order parameter drives temporal changes in the parameter θ (equation (4)), thereby altering the shape of the effective free energy over time. Specifically, above a critical size, as the uninformed ants enter their 'ordered' phase, the effective free energy $W(v,\theta)$ develops two non-zero minima (Fig. 6b).

In the direction $\theta=0$ towards the nest, $W(v,0)$ is symmetric, but a small perturbation leads to symmetry breaking and the group starts moving sideways with a speed that corresponds to either one of the minima (Fig. 6b, top-left frame). As the group moves away from $\theta=0$, the tangential projection of the informed ants' force, G, increases and the effective energy ceases to be symmetric (Fig. 6b, top-right frame). Eventually, the occupied minimum of $W(v,\theta)$ loses its stability (Fig. 6b, bottom-left frame) and the system jumps to a speed in the opposite direction (Fig. 6b, bottom-right frame). This process leads to deterministic relaxation oscillations along a limit cycle. Thus, the change of directionality does not necessitate the attachment of new informed ants. This phenomenon was also observed in experiments with a cul-de-sac geometry, where backward motion was often initiated without the attachment of a new ant[46].

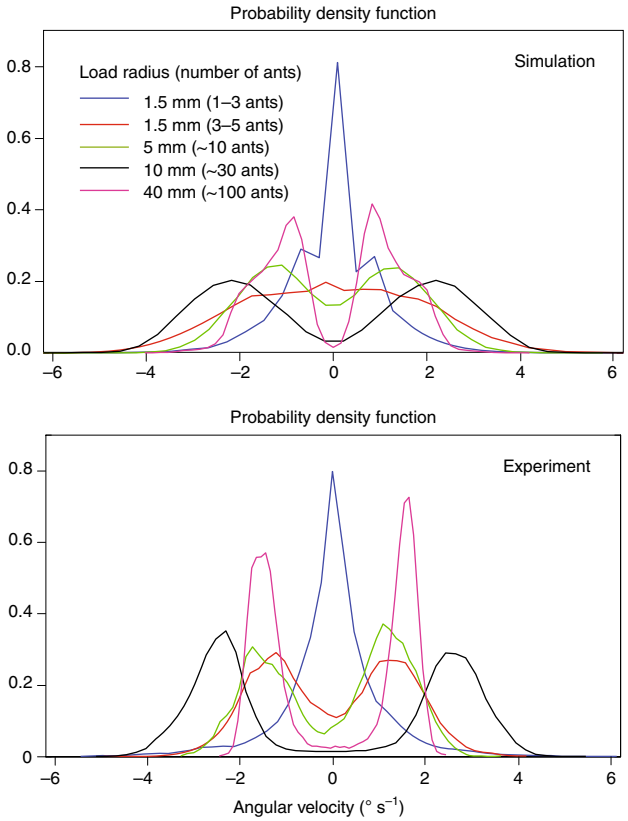

Fig. 5 | Increasing system size transits the system between order and disorder in experiment and simulation. Distributions of angular velocities of a constrained load. Both simulation (top panel) and experimental results (bottom) depict a transition from random fluctuations around $\theta=0$ (uni-modal distributions) to large-scale oscillations (bi-modal distributions) with growing load size (as in the legend).

The bifurcation diagram of equation (4) is shown Fig. 6c. In addition to the local Hopf bifurcation, the model predicts a heteroclinic bifurcation into complete rotations. To test for this motion in experiments, the string was replaced by a rod to prevent inward radial motion. Indeed, as shown in Fig. 6d,e the rod-constrained system exhibits complete rotations, which are more persistent for larger cargoes[34]. Finally, the experimentally observed velocity extrema are at the predicted $\theta=\pm 90°$, unlike the case of rotations under gravity where the extrema in the velocity are at $\theta=0, 180°$ (Fig. 6e).

These findings have implications on biologically relevant aspects of this system: the same model can explain both the free and the constrained motions and this suggests that the rules that ants follow near an obstacle are the same as those obeyed during unconstrained motion. The excursions that the group takes when encountering an obstacle can be seen as an example of collective problem solving, as they help circumvent the obstacle and emerge without the individual ants realizing that they are blocked.

The inclusion of an external constraint has allowed for a straightforward distinction between two different models of cooperation. This physical insight suggests a practical research path that can be

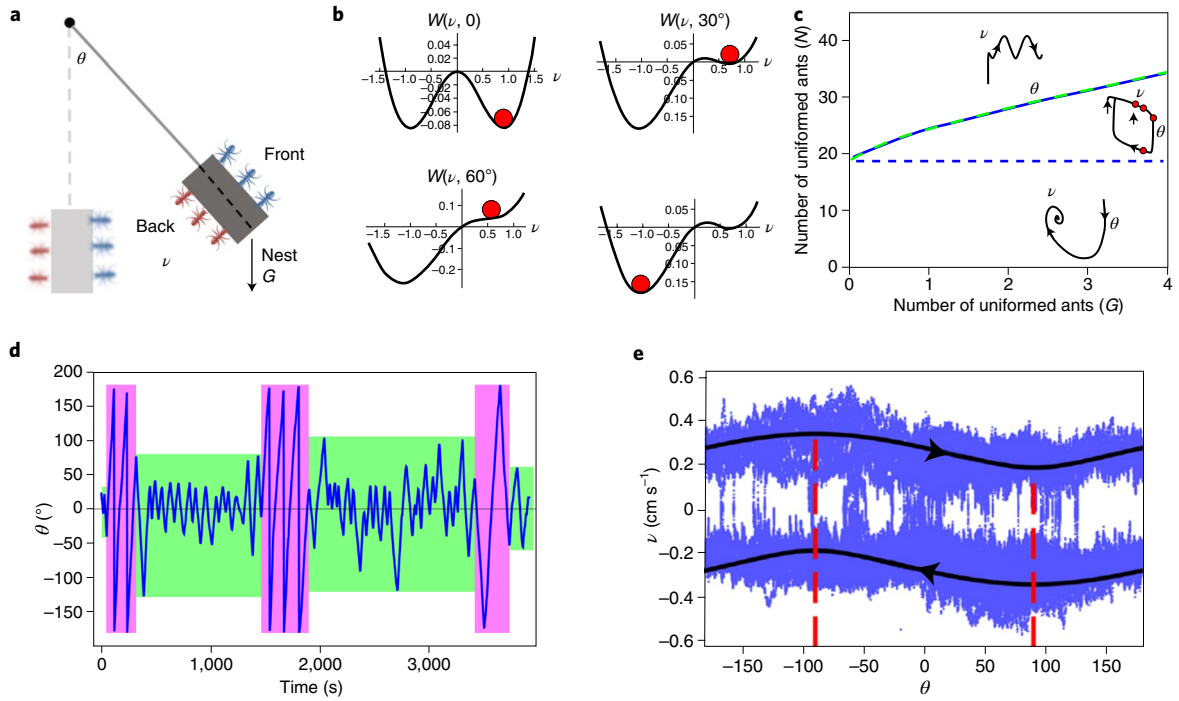

Fig. 6 | Phase transitions under constrained motion. a, A constrained version of the simplified coupled model. The motion of the load is described by the parameters (θ, v). The pull of informed ants is modelled as a `gravitational' pull, G, towards the nest. **b**, The effective free energy, $W(\theta, v)$, as a function of v and at four θ locations along the trajectory (marked by red dots, ordered in a clockwise fashion, in **c**). The red disc in each of the frames depicts the order parameter, v, of the cargo. **c**, Calculated phase diagram of the constrained system as a function of the number of uninformed, N, and informed, G, ants. From bottom to top, the diagram displays a non-ordered phase, an oscillatory phase and a phase of complete rotations. **d**, Experimental results demonstrating a system that occasionally alternates between the oscillatory phase (green background) and the full rotation phase (pink background). **e**, Experimental (blue) and theoretical (black) phase-space trajectories for complete rotations. The red dashed lines denote extremal angles, ±90°, and $\theta = 0$ is the nest direction.

expected to expand our understanding of social insect behaviour and its evolution. Namely, we propose an empirical survey in which cooperatively carrying ant species[23,24] are subjected to constrained transport and the degree of oscillatory motion is measured. Species may then be arranged according to similarities in their collective trajectories[23,35]. Correlating these with phylogenetic and environmental similarities may then have implications for the evolution and ecology of cooperation by social insects.

Figure 7 presents some preliminary steps in this direction. When confronted with a tethered load, ants of the species *Pheidole pallidula* exhibit large-scale oscillations that support a coupled model for this species. The similarity of these oscillations to those of *P. longicornis* (Fig. 4a,b) demonstrates the generality of our model. Further, *P. pallidula* is phylogenetically distant from *P. longicornis*—the former is in the Myrmicinae subfamily, the latter in the Formicinae subfamily—but inhabits a similar biological niche, which may suggest convergent evolution[61,62] towards coupled transport in these two species.

Ants as interacting particles

Ants who take part in collective transport participate in a large-scale process whereby their individual actions act to coordinate them into a single, cooperative entity. This coordination is achieved via physical interactions in which a carrier ant senses the force generated by the entire carrying group and reacts by aligning its pull with this collective 'opinion'. Although this trait of 'going with the flow' is strongly associated with ant behaviour, it has also been shown that, in complex environments, some degree of independence is useful[63]. Indeed, this principle carries over to cooperative transport behaviour where the alignment of carriers is crucial but, nevertheless, imperfect.

The carrying ant groups exhibit the necessary ingredients to support a phase transition in a many-body system. Importantly, group size serves as a control parameter that transitions the group between different phases of motion. Small carrying teams display a disordered phase, which is characterized by uncoordinated tug-of-war[33], whereas large ant groups coordinate into an ordered phase, characterized by more ballistic motion. A similar transition has previously been demonstrated in the collective motion of locusts where the density of the swarm serves as a control parameter[9]. The effect of group size in ants stands in contrast to bird flocks[4] and midge swarms[41], which are thought to self-tune to remain near the critical point, regardless of group size. This property of the ant system provides an experimental advantage as it allows for a study of cooperative transport in its ordered and disordered phases, as well as in the transition region between them.

The navigational capabilities of carrying ants may be compromised in comparison to those of freely moving ants[33]. For example, carrying a large load may obstruct sensory inputs as well as hamper any idiothetic orientation mechanisms[64]. To maintain an influx of orientational information and correctly steer towards the nest, the group must therefore maintain a high degree of responsiveness to the motions of incoming ants equipped with new information. Interestingly, the same physical principles that drive the transition into a coordinated carrying phase also provide the mechanism for high responsiveness. It was found that the range of sizes of naturally occurring cargoes places the ants near the critical point of the order–disorder transition. In this critical regime, the susceptibility of the system to small external perturbations is maximal. A newly arrived and informed ant provides this external pull, and the group readily responds by altering its direction of motion to follow this

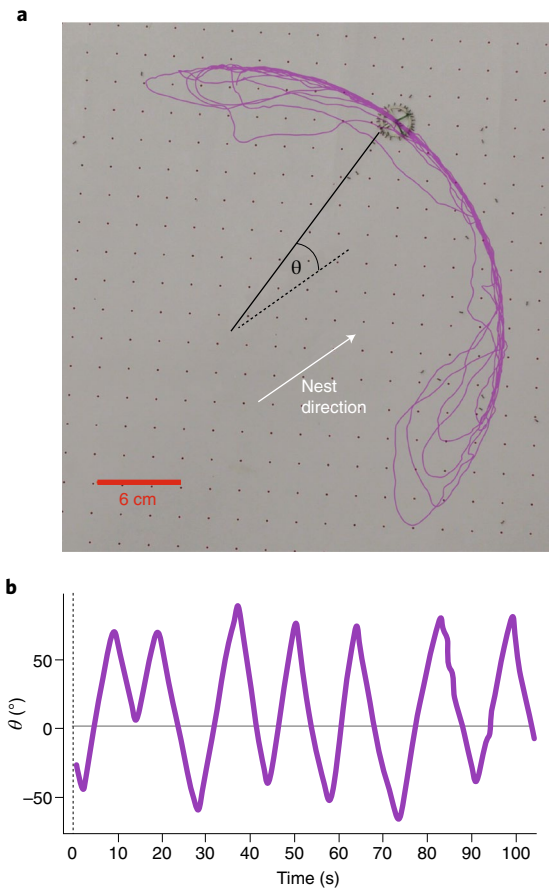

Fig. 7 | Oscillatory motion in a different species. a, The motion of cooperatively carrying *P. pallidula* ants constrained by a thin tether (black line). **b**, Time series of the load's motion. A black dashed line marks the onset of oscillatory motion. The angle, θ, is measured relative to the direction of the nest.

transient leader[33]. Collective carrying by ants therefore presents another striking example in which natural selection optimizes the performance of the group by positioning it near a phase transition[4,41,65,66]. Intriguingly, it has been further suggested that residing at criticality enables an interacting system to maximize its computational capabilities[67].

In this review, we have emphasized the usefulness of simplified theoretical models in promoting our understanding of complex biological systems. Clearly ants are not particles: they do not take binary decisions using Boltzmann-like statistics, and their interactions with each other may be highly intricate. The models for the special case of cooperative transport, as presented above, employ the following simplifications: a dichotomous separation between informed and uninformed ants, a rigid load assumption and no role for the scent trail known to exist[47]. Although these simplifications are not completely realistic, it was previously shown that relaxing some of these assumptions does not strongly impact the predictions of the model[33]. More importantly, the success of these models in qualitatively and quantitatively describing experimental results, as well as predicting new phenomena subsequently verified by experiments, demonstrates the strength of abstract modelling.

The understanding of ant cooperative transport has implications for other collective biological phenomena. First, there are analogous examples of cooperative transport systems on very different length scales. Examples include transport of intracellular cargoes by teams of molecular motors along one dimension[51,52] and collective cell motion[6,68,69]. Second, there is an interesting analogy between the carrying ants and neural network systems. Specifically, the model of interacting carrier ants around a circular load can be mapped to the well-known 'ring model'[70,71]. In both systems, incoming information results in an angularly defined response. In the case of the ring model, the new information is visual, and encoded by electric potentials, whereas the pull of newly attached ants carries the orientational information in the case of cooperative transport. Third, the lessons learned from ants may find technological applications for the design of cooperative transport in robotic systems[72–76]. Finally, the interplay between conformism, individuality and leadership in ants has been suggested to have analogies in human societies[77–79].

This work demonstrates the strength of statistical physics, combined with quantitative experiments, in deciphering the underlying rules that govern collective animal behaviour, even if direct measurements of the interactions within the group remain elusive[36]. The relative success of this approach raises the question of how far statistical physics modelling can take us when describing such a complex biological system[37,80]. In the context of cooperative transport, the answer to this question is perplexing. The collective behaviour of ants is strongly dictated by physical principles in which ants play the role of simple coupled particles. Interestingly, this coupled system is maximally responsive to the complex decisions and information provided by few navigationally competent individuals. These informed ants, although crucial for understanding the collective motion, lie outside the realm of simple interacting particle models.

Received: 19 July 2017; Accepted: 8 March 2018;
Published online: 14 May 2018

References

1. Vicsek, T., Czirók, A., Ben-Jacob, E., Cohen, I. & Shochet, O. Novel type of phase transition in a system of self-driven particles. *Phys. Rev. Lett.* **75**, 1226 (1995).
2. Toner, J. & Tu, Y. Long-range order in a two-dimensional dynamical XY model: how birds fly together. *Phys. Rev. Lett.* **75**, 4326–4329 (1995).
3. Toner, J. & Tu, Y. Flocks, herds, and schools: A quantitative theory of flocking. *Phys. Rev. E* **58**, 4828–4858 (1998).
4. Cavagna, A. et al. Scale-free correlations in starling flocks. *Proc. Natl Acad. Sci. USA* **107**, 11865–11870 (2010).
5. Vicsek, T. Universal patterns of collective motion from minimal models of flocking. In *Proc. 2nd IEEE International Conference on Self-Adaptive and Self-Organizing Systems, SASO 2008* 3–11 (2008).
6. Vicsek, T. & Zafeiris, A. Collective motion. *Phys. Rep.* **517**, 71–140 (2012).
7. Ariel, G. & Ayali, A. Locust collective motion and its modeling. *PLoS Comput. Biol.* **11**, e1004522 (2015).
8. Procaccini, A. et al. Propagating waves in starling, *Sturnus vulgaris*, flocks under predation. *Anim. Behav.* **82**, 759–765 (2011).
9. Buhl, J. et al. From disorder to order in marching locusts. *Science* **312**, 1402–1406 (2006).
10. Parrish, J. K., Viscido, S. V. & Grunbaum, D. Self-organized fish schools: an examination of emergent properties. *Biol. Bull.* **202**, 296–305 (2002).
11. Tunstrøm, K. et al. Collective states, multistability and transitional behavior in schooling fish. *PLoS Comput. Biol.* **9**, e1002915 (2013).
12. Pearce, D. J., Miller, A. M., Rowlands, G. & Turner, M. S. Role of projection in the control of bird flocks. *Proc. Natl Acad. Sci. USA* **111**, 10422–10426 (2014).
13. Rosenthal, S. B., Twomey, C. R., Hartnett, A. T., Wu, H. S. & Couzin, I. D. Revealing the hidden networks of interaction in mobile animal groups allows prediction of complex behavioral contagion. *Proc. Natl Acad. Sci. USA* **112**, 4690–4695 (2015).
14. Dussutour, A., Fourcassie, V., Helbing, D. & Deneubourg, J.-L. Optimal traffic organization in ants under crowded conditions. *Nature* **428**, 70–73 (2004).
15. Bazazi, S. et al. Collective motion and cannibalism in locust migratory bands. *Curr. Biol.* **18**, 735–739 (2008).
16. Liao, J. C., Beal, D. N., Lauder, G. V. & Triantafyllou, M. S. Fish exploiting vortices decrease muscle activity. *Science* **302**, 1566–1569 (2003).
17. Morgan, E. D. Trail pheromones of ants. *Physiol. Entomol.* **34,** 1–17 (2009).
18. Ben-Jacob, E. et al. Generic modelling of cooperative growth patterns in bacterial colonies. *Nature* **368**, 46 (1994).

19. Darmon, M., Brachet, P. & Da Silva, L. Chemotactic signals induce cell differentiation in dictyostelium discoideum. *Proc. Natl Acad. Sci. USA* **72**, 3163–3166 (1975).
20. Cvikel, N. et al. Bats aggregate to improve prey search but might be impaired when their density becomes too high. *Curr. Biol.* **25**, 206–211 (2015).
21. Gorbonos, D. et al. Long-range acoustic interactions in insect swarms: an adaptive gravity model. *New J. Phys.* **18**, 073042 (2016).
22. Ballerini, M. et al. Interaction ruling animal collective behavior depends on topological rather than metric distance: Evidence from a field study. *Proc. Natl Acad. Sci. USA* **105**, 1232–1237 (2008).
23. Czaczkes, T. J. & Ratnieks, F. L. W. Cooperative transport in ants (Hymenoptera: Formicidae) and elsewhere. *Myrmecol. News* **18**, 1–11 (2013).
24. McCreery, H. & Breed, M. Cooperative transport in ants: a review of proximate mechanisms. *Insect Soc.* **61**, 99–110 (2014).
25. Moffett, M. W. Cooperative food transport by an Asiatic ant. *Natl Geogr. Res.* **4**, 386–394 (1988).
26. Hölldobler, B. & Wilson, E. O. *The Ants* (Harvard Univ. Press, Cambridge, MA, 1990).
27. Sudd, J. H. The transport of prey by ants. *Behaviour* **25**, 234–271 (1965).
28. Buffin, A. & Pratt, S. Cooperative transport by the ant *Novomessor cockerelli*. *Insectes Soc.* **63**, 429–438 (2016).
29. Franks, N. R. Teams in social insects: group retrieval of prey by army ants (*Eciton burchellii*, Hymenoptera: Formicidae). *Behav. Ecol. Sociobiol.* **18**, 425–429 (1986).
30. Moffett, M. W. *Sociobiology of the Ants of the Genus* Pheidologeton (Harvard Univ. Press, Cambridge, MA, 1988).
31. Czaczkes, T. & Ratnieks, F. L. Simple rules result in the adaptive turning of food items to reduce drag during cooperative food transport in the ant *Pheidole oxyops*. *Insectes Soc.* **58**, 91–96 (2011).
32. Berman, S., Lindsey, Q., Sakar, M. S., Kumar, V. & Pratt, S. Study of group food retrieval by ants as a model for multi-robot collective vtransport strategies. *Robot. Proc.* https://doi.org/10.15607/RSS.2010.VI.033 (2010).
33. Gelblum, A. et al. Ant groups optimally amplify the effect of transiently informed individuals. *Nat. Commun.* **6**, 7729 (2015).
34. Gelblum, A., Pinkoviezky, I., Fonio, E., Gov, N. S. & Feinerman, O. Emergent oscillations assist obstacle negotiation during ant cooperative transport. *Proc. Natl Acad. Sci. USA* **113**, 14615–14620 (2016).
35. McCreery, H. A comparative approach to cooperative transport in ants: individual persistence correlates with group coordination. *Insectes Soc.* **64**, 535–547 (2017).
36. Berman, S., Lindsey, Q., Sakar, M. S., Kumar, V. & Pratt, S. C. Experimental study and modeling of group retrieval in ants as an approach to collective transport in swarm robotic systems. *Proc. IEEE* **99**, 1470–1481 (2011).
37. Bialek, W. et al. Statistical mechanics for natural flocks of birds. *Proc. Natl Acad. Sci. USA* **109**, 4786–4791 (2012).
38. Mora, T. & Bialek, W. Are biological systems poised at criticality? *J. Stat. Phys.* **144**, 268–302 (2011).
39. Bialek, W. et al. Social interactions dominate speed control in poising natural flocks near criticality. *Proc. Natl Acad. Sci. USA* **111**, 7212–7217 (2014).
40. Hidalgo, J. et al. Information-based fitness and the emergence of criticality in living systems. *Proc. Natl Acad. Sci. USA* **111**, 10095–10100 (2014).
41. Attanasi, A. et al. Finite-size scaling as a way to probe near-criticality in natural swarms. *Phys. Rev. Lett.* **113**, 238102 (2014).
42. Sumpter, D., Buhl, J., Biro, D. & Couzin, I. Information transfer in moving animal groups. *Theory Biosci.* **127**, 177–186 (2008).
43. Peeters, C. & De Greef, S. Predation on large millipedes and self-assembling chains in *Leptogenys* ants from Cambodia. *Insectes Soc.* **62**, 471–477 (2015).
44. Czaczkes, T. J., Vollet-NetoA. & Ratnieks, F. L. Prey escorting behavior and possible convergent evolution of foraging recruitment mechanisms in an invasive ant. *Behav. Ecol.* **24**, 1177–1184 (2013).
45. Trager, J. C. A revision of the genus *Paratrechina* (Hymenoptera: Formicidae) of the continental united states. *Sociobiology* **8**, 49–162 (1984).
46. McCreery, H. F., Dix, Z. A., Breed, M. D. & Nagpal, R. Collective strategy for obstacle navigation during cooperative transport by ants. *J. Exp. Biol.* **219**, 3366–3375 (2016).
47. Fonio, E. et al. A locally-blazed ant trail achieves efficient collective navigation despite limited information. *eLife* **5**, e20185 (2016).
48. Simons, A. M. Many wrongs: the advantage of group navigation. *Trends Ecol. Evol.* **19**, 453–455 (2004).
49. Galton, F. Vox populi (the wisdom of crowds). *Nature* **75**, 450–451 (1907).
50. Faria, J. J., Codling, E. A., Dyer, J. R., Trillmich, F. & Krause, J. Navigation in human crowds; testing the many-wrongs principle. *Anim. Behav.* **78**, 587–591 (2009).
51. Hancock, W. O. Bidirectional cargo transport: moving beyond tug of war. *Nat. Rev. Mol. Cell Biol.* **15**, 615–628 (2014).
52. Hendricks, A. G. et al. Motor coordination via a tug-of-war mechanism drives bidirectional vesicle transport. *Curr. Biol.* **20**, 697–702 (2010).
53. Mobilia, M. Does a single zealot affect an infinite group of voters? *Phys. Rev. Lett.* **91**, 028701 (2003).
54. Hartnett, A. T., Schertzer, E., Levin, S. A. & Couzin, I. D. Heterogeneous preference and local nonlinearity in consensus decision making. *Phys. Rev. Lett.* **116**, 038701 (2016).
55. Wehner, R. Desert ant navigation: how miniature brains solve complex tasks. *J. Comp. Physiol. A* **189**, 579–588 (2003).
56. Razin, N., Eckmann, J.-P. & Feinerman, O. Desert ants achieve reliable recruitment across noisy interactions. *J. R. Soc. Interface* **10**, 20130079 (2013).
57. Robson, S. K. & Traniello, J. F. Transient division of labor and behavioral specialization in the ant *Formica schaufussi*. *Naturwissenschaften* **89**, 128–131 (2002).
58. Feinerman, O. in *Landscapes of Collectivity in the Life Sciences* (eds Gissis, S. et al.) Ch. 4 (MIT Press, Cambridge, MA, 2018).
59. Ludwig, M. & Marquardt, F. Quantum many-body dynamics in optomechanical arrays. *Phys. Rev. Lett.* **111**, 073603 (2013).
60. Chan, C.-K., Lee, T. E. & Gopalakrishnan, S. Limit-cycle phase in driven-dissipative spin systems. *Phys. Rev. A* **91**, 051601 (2015).
61. D'Ettorre, P. & Heinze, J. Sociobiology of slave-making ants. *Acta Ethol.* **3**, 67–82 (2001).
62. Ward, P. S. & Branstetter, M. G. The acacia ants revisited: convergent evolution and biogeographic context in an iconic ant/plant mutualism. *Proc. R. Soc. B* **284**, 1850 (2017).
63. Deneubourg, J.-L., Pasteels, J. M. & Verhaeghe, J.-C. Probabilistic behaviour in ants: a strategy of errors? *J. Theor. Biol.* **105**, 259–271 (1983).
64. Müller, M. & Wehner, R. Path integration in desert ants, *Cataglyphis fortis*. *Proc. Natl Acad. Sci. USA* **85**, 5287–5290 (1988).
65. Rauch, E. M., Millonas, M. M. & Chialvo, D. R. Pattern formation and functionality in swarm models. *Phys. Lett. A* **207**, 185–193 (1995).
66. Daniels, B. C., Krakauer, D. C. & Flack, J. C. Control of finite critical behaviour in a small-scale social system. *Nat. Commun.* **8**, 14301 (2017).
67. Langton, C. G. Computation at the edge of chaos: phase transitions and emergent computation. *Phys. D* **42**, 12–37 (1990).
68. Kabla, A. J. Collective cell migration: leadership, invasion and segregation. *J. R. Soc. Interface* **9**, 3268–3278 (2012).
69. Szabo, B. et al. Phase transition in the collective migration of tissue cells: experiment and model. *Phys. Rev. E* **74**, 061908 (2006).
70. Goldberg, J. A., Rokni, U. & Sompolinsky, H. Patterns of ongoing activity and the functional architecture of the primary visual cortex. *Neuron* **42**, 489–500 (2004).
71. Green, J. et al. A neural circuit architecture for angular integration in *Drosophila*. *Nature* **546**, 101–106 (2017).
72. Kube, C. R. & Bonabeau, E. Cooperative transport by ants and robots. *Robot. Auton. Syst.* **30**, 85–101 (2000).
73. Iqbal, T., Rack, S. & Riek, L. D. Movement coordination in human–robot teams: A dynamical systems approach. *IEEE Trans. Robot.* **32**, 909–919 (2016).
74. Wilson, S. et al. Design of ant-inspired stochastic control policies for collective transport by robotic swarms. *Swarm Intell.* **8**, 303–327 (2014).
75. Wang, Z. & Schwager, M. in *Distributed Autonomous Robotic Systems* (eds Chong, N.-Y., Cho, Y.-J.) 135–149 (Springer, Berlin, Heidelberg, 2016).
76. Wang, Z. & Schwager, M. Kinematic multi-robot manipulation with no communication using force feedback. In *Proc. 2016 IEEE International Conference on Robotics and Automation (ICRA)* 427–432 (IEEE, 2016).
77. Realpe-Gómez, J., Andrighetto, G., Nardin, G. & Montoya, J. A. Balancing selfishness and norm conformity can explain human behavior in large-scale Prisoner's Dilemma games and can poise human groups near criticality. Preprint at https://arxiv.org/abs/1608.01291 (2016).
78. Lehmann, O. F. *Situational Project Management: The Dynamics of Success and Failure* (CRC Press, Boca Raton, FL, 2016).
79. Puranam, P. When will we stop studying innovations in organizing, and start creating them? *Innovation* **19**, 5–10 (2017).
80. Detrain, C. & Deneubourg, J.-L. Self-organized structures in a superorganism: do ants "behave" like molecules? *Phys. Life Rev.* **3**, 162–187 (2006).
81. Gillespie, D. T. Exact stochastic simulation of coupled chemical reactions. *J. Phys. Chem.* **81**, 2340–2361 (1977).

Acknowledgements

We would like to thank Ehud Altman for useful discussions. N.S.G. is the incumbent of the Lee and William Abramowitz Professorial Chair of Biophysics and is supported by the Israel Science Foundation (ISF) (grant no. 580/12), and Minerva Foundation research grant no. 712601. O.F. is the incumbent of the Shloimo and Michla Tomarin Career Development Chair and was supported by the Israeli Science Foundation grant 833/15, and the European Research Council under the European Union's Horizon 2020 research and innovation program (grant agreement no. 770964), and the Clore Duffield Foundation. E.F. is the incumbent of the Tom Beck Research Fellow Chair in the Physics of Complex Systems.

Author contributions

All authors have contributed to the writing and figure preparation of this review.

Competing interests

The authors declare no competing interests.

Additional information

Reprints and permissions information is available at www.nature.com/reprints.

Correspondence should be addressed to O.F.

Publisher's note: Springer Nature remains neutral with regard to jurisdictional claims in published maps and institutional affiliations.